

Impurity Effect as a Probe for the Gap Function in the Filled Skutterudite Compound Superconductor $\text{PrOs}_4\text{Sb}_{12}$: Sb-NQR Study

Masahide NISHIYAMA, Takayuki KATO, Hitoshi SUGAWARA¹, Daisuke KIKUCHI², Hideyuki SATO², Hisatomo HARIMA³, and Guo-qing ZHENG

Department of Physics, Okayama University, Okayama 700-8530, Japan

¹*Department of Mathematical and Natural Sciences, Faculty of Integrated Arts and Sciences, The University of Tokushima, Tokushima 770-8502, Japan*

²*Department of Physics, Graduate School of Science, Tokyo Metropolitan University, Hachioji 192-0397, Japan*

³*Department of Physics, Kobe University, Kobe 657-8501, Japan*

We have carried out nuclear quadrupole resonance (NQR) measurements in the filled skutterudite compounds $\text{Pr}(\text{Os}_{1-x}\text{Ru}_x)_4\text{Sb}_{12}$ ($x = 0.1, 0.2$), in order to gain insights into the symmetry of the superconducting gap function. Upon replacing Os with Ru, the spin-lattice relaxation rate $1/T_1$ becomes proportional to temperature (T) at low T far below T_c , and the magnitude of $(1/T_1T)_{low-T}$ increases with increasing Ru content. These results indicate that a finite density of states is induced at the Fermi level by the impurity, and thus suggest that there exist nodes in the gap function of $\text{PrOs}_4\text{Sb}_{12}$.

KEYWORDS: filled skutterudite, Heavy fermion, superconductivity, impurity effect, nuclear quadrupole resonance, residual DOS

The superconductivity at $T_c=1.85$ K discovered in the filled skutterudite compound $\text{PrOs}_4\text{Sb}_{12}$ has attracted much attention.^{1,2} This is the first Pr-based heavy fermion superconductor, in which the heavy mass has been suggested by the large specific heat jump $\Delta C/T_c \sim 500$ mJ/K²·mol at T_c ,^{1,2} and directly confirmed by de Haas-van Alphen (dHvA) experiments.³ The crystal electric field (CEF) ground state is a Γ_1 singlet, which is separated by the first excited state of the $\Gamma_4^{(2)}$ triplet by a gap of $\Delta_{CEF}=10$ K.⁴⁻⁹ Because of this small Δ_{CEF} , the role of quadrupole moment fluctuations arising from the $\Gamma_4^{(2)}$ state has attracted much attention. It has been speculated that the interaction between the quadrupolar moments and the conduction-electron charges may be responsible for the heavy mass, thus representing a charge-scattering version of the Kondo effect.¹⁰ The contrasting behavior that the isostructural compound $\text{PrRu}_4\text{Sb}_{12}$ with $\Delta_{CEF}=70$ K has a much smaller m^* ,^{11,12} has increased such expectation.

One of the first steps toward understanding the Pr-based heavy fermions may be the determination of the gap symmetry of the superconductivity. Previous nuclear quadrupole resonance (NQR) measurements have revealed the unconventional nature of the supercon-

ductivity.¹³ No coherence peak was found in the spin-lattice relaxation rate $1/T_1$ just below T_c , which suggests non-BCS-type superconductivity and is in contrast to the s -wave behavior subsequently observed in $\text{PrRu}_4\text{Sb}_{12}$.¹⁴ At low temperatures, $1/T_1$ does not follow a power-law T -dependence, which is in contrast to the observation of a T^3 variation in other known heavy fermion superconductors.¹⁵ Together with the exponential decrease in the penetration depth found by muon spin relaxation,¹⁶ it has been suggested that the superconducting gap is isotropic. However, oscillations with respect to the magnetic field angle have been found in angle-resolved thermal conductivity measurements, which suggests that the gap is anisotropic.¹⁷

In this study, we use an impurity as a probe for the gap function. We replace Os with Ru, and study its effect on the superconducting density of states (DOS) using the NQR technique. It has been known for some time that a non-magnetic impurity is a powerful "smoking gun" for the gap function. In s -wave superconductors, a paramagnetic impurity produces a bound state within the gap (Yu-Shiba state),^{18,19} and non-magnetic impurities smear out the gap anisotropy, if any.²⁰ In contrast, if there are nodes in the gap function, a finite DOS is brought about at the Fermi level,^{21,22} which can be detected experimentally.¹⁵

Single crystals of $\text{Pr}(\text{Os}_{1-x}\text{Ru}_x)_4\text{Sb}_{12}$, ($x=0.1$ and 0.2) were grown by the Sb-flux method. T_c 's are 1.6 K and 1.4 K for $x=0.1$ and 0.2 , respectively, in agreement with those previously reported.^{23,24} For NQR measurements, the single crystals were powdered in order to allow the radio-frequency magnetic field to penetrate into the sample. The NQR measurements were performed by using a phase coherent spectrometer. The spin-lattice relaxation rate, $1/T_1$, for ^{123}Sb were measured using the saturation-recovery method. Data below 1.4 K were collected using a $^3\text{He}/^4\text{He}$ dilution refrigerator.

Figure 1 shows the NQR spectra for the $x=0.1$ and 0.2 samples. For comparison, the data for the two end-member compounds^{13,14} are also shown in Figs 1(a) and 1(d). In the Ru-doped samples, in addition to the spectrum peaks that are located at the same positions as those for pure $\text{PrOs}_4\text{Sb}_{12}$, there appear new sets of peaks that are characterized by $\nu_Q=26$ MHz and the asymmetry parameter $\eta=0.43$ for ^{123}Sb . Here, ν_Q and η are defined as $\nu_Q \equiv \nu_z = \frac{3}{2I(2I-1)\hbar} e^2 Q \frac{\partial^2 V}{\partial z^2}$ and $\eta = |\nu_x - \nu_y|/\nu_z$ with Q being the nuclear quadrupolar moment and $\frac{\partial^2 V}{\partial \alpha^2}$ ($\alpha = x, y, z$) being the electric field gradient at the position of the nucleus.²⁵ It should be emphasized that these peaks (labelled as "peaks 2" in Table I) are different from those for pure $\text{PrRu}_4\text{Sb}_{12}$. These new peaks are due to the alloying effect, which indicates that the alloying is homogenous and there is no phase separation. Such a feature has been seen before in other heavy fermion compounds. For example, in Ir-doped CeRhIn_5 , upon replacing Rh with Ir, there emerges a new set of NQR peaks that is different from that for CeRhIn_5 or CeIrIn_5 .²⁶ Nonetheless, $1/T_1$ measured at the new set of peaks shows the same T -dependence as that measured at those corresponding to CeRhIn_5 or CeIrIn_5 , indicating that the new set

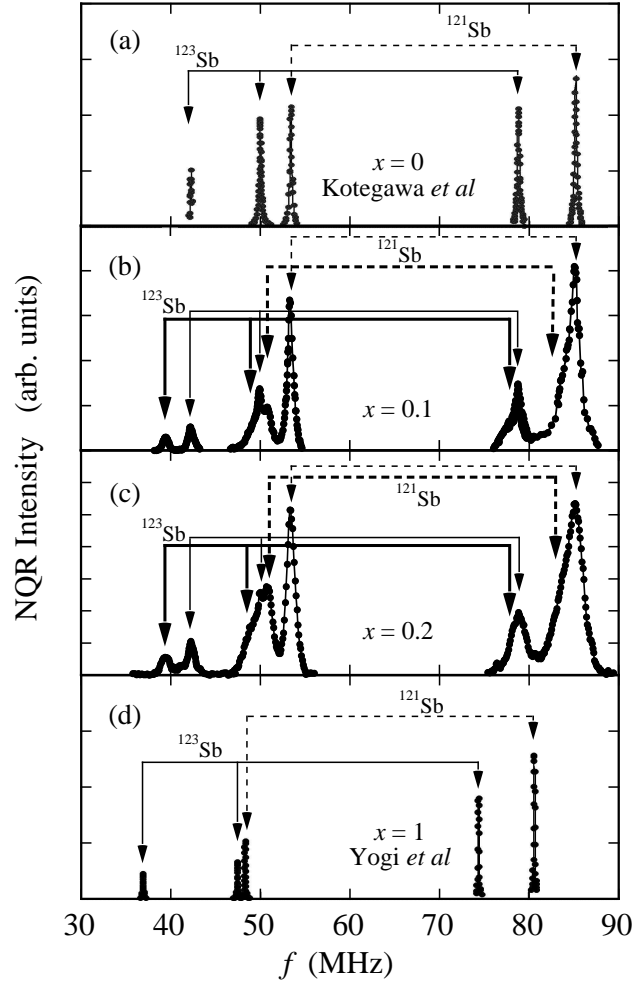


Fig. 1. Sb-NQR spectra of $\text{Pr}(\text{Os}_{1-x}\text{Ru}_x)_4\text{Sb}_{12}$ at 4.2 K. The data for $x = 0$ and $x = 1$ are from Kotegawa *et al.*¹³ and Yogi *et al.*¹⁴ In (b) and (c), the spectra indicated by the thin solid lines (broken lines) correspond to ^{123}Sb (^{121}Sb) signals seen in $\text{PrOs}_4\text{Sb}_{12}$, while the spectra indicated by the thick markers are the new sets arising from Ru doping.

of peaks is not due to phase-separated regions but rather to the homogenous alloying.

The nuclear spin-lattice relaxation rate $1/T_1$ was measured at the peaks at 49.9 MHz ($\pm 3/2 \leftrightarrow \pm 5/2$ transition) and 42.2 MHz ($\pm 1/2 \leftrightarrow \pm 3/2$ transition). Both measurements yield the same results. Even for $x=0.2$, no influence on T_1 due to the overlapping of the ^{121}Sb line was seen in the measurements at the 49.9 MHz peak, probably because the H_1 we used for observing the echo is much smaller than the frequency difference between the ^{121}Sb and ^{123}Sb peaks, which is about 0.8 MHz, and the ^{121}Sb peak has a small full width at half maximum (FWHM) of 0.5 MHz. Above $T \sim 100$ K, the nuclear magnetization can be fitted excellently using the expected theoretical rate equation.²⁷ However, below $T \sim 100$ K, it cannot be fitted using the theoretical curve with a single component of T_1 . This is also true at the peak at 42.2

Table I. NQR frequency ν_Q and asymmetric parameter η for ^{123}Sb in $\text{Pr}(\text{Os}_{1-x}\text{Ru}_x)_4\text{Sb}_{12}$. Also shown are the CEF gap Δ_{CEF} and the heavy quasiparticle enhancement factor β (see text).

x	Peaks 1		Peaks 2		β	Δ_{CEF} (K)
	ν_Q (MHz)	η	ν_Q (MHz)	η		
0	26.8	0.41	—	—	26.7	8
0.1	26.8	0.41	26	0.43	16	10
0.2	26.8	0.41	26	0.43	11	13
1	25.2	0.46	—	—	—	—

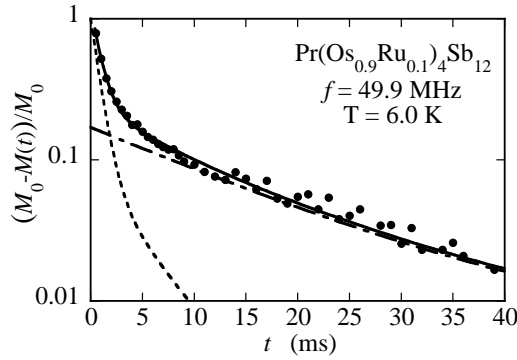


Fig. 2. Nuclear magnetization recovery curve. The broken and dot-dashed curves indicate the recovery curves due to the fast and slow relaxation components, respectively. The solid curve indicates the sum of the two components.

MHz that is free from overlapping by other transition lines. Figure 2 shows the decay curve of the nuclear magnetization at $T=6$ K. As will become clearer later, the inhomogeneous T_1 is an intrinsic property of the alloyed samples. The one-component behavior for $T \geq 100$ K is rather a coincidence, since T_1 is the same for both $\text{PrOs}_4\text{Sb}_{12}$ and $\text{PrRu}_4\text{Sb}_{12}$.

We then attempt to fit the low- T nuclear magnetization with two T_1 components, namely,

$$\frac{M_0 - M(t)}{M_0} = \sum_{i=S,L} a_i \left[0.0762 \exp\left(-\frac{3t}{T_1^S}\right) + 0.0146 \exp\left(-\frac{8.9t}{T_1^L}\right) + 0.9092 \exp\left(-\frac{17.3t}{T_1^L}\right) \right] \quad (1)$$

where T_1^S means the short component due to fast relaxation, and T_1^L , the long component due to slow relaxation. The solid curve in Fig. 2 shows such fitting for $x=0.1$, with $a_S=0.8$ and $a_L=0.2$ that do not depend on temperature appreciably.

We first discuss the main component, $1/T_1^S$, whose temperature dependence is shown in Fig. 3. Compared to the results for the end-member compounds, several trends can be seen. First, above $T \sim 100$ K, there is only one component of T_1 (namely, $T_1^S = T_1^L$), and the data

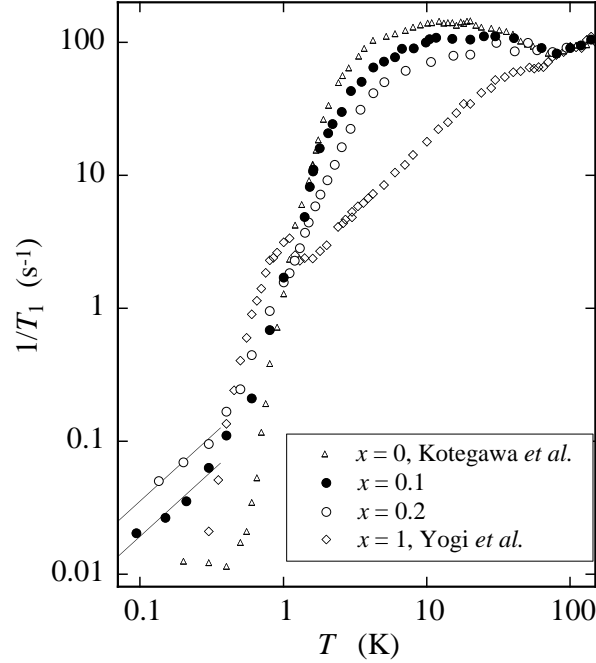


Fig. 3. Temperature dependence of $1/T_1^S$ in $\text{Pr}(\text{Os}_{1-x}\text{Ru}_x)_4\text{Sb}_{12}$ ($x = 0.1, 0.2$). Data for $\text{PrOs}_4\text{Sb}_{12}$ ¹³ and $\text{PrRu}_4\text{Sb}_{12}$, which is a BCS superconductor,¹⁴ are also shown for comparison. The straight lines indicate the $T_1T = \text{const}$ relations.

for all x merge into a same line. This suggests that the relaxation at high T is *not* governed by the electronic state that is sensitive to the transition metal element,²⁸ but due to other degree of freedom. Second, below $T \sim 100$ K, $1/T_1^S$ is close to that for pure $\text{PrOs}_4\text{Sb}_{12}$, but decreases as x increases. Since the slow component $1/T_1^L$ is very close to that for pure $\text{PrRu}_4\text{Sb}_{12}$, as will be shown later, we consider that $1/T_1^S$ originates from the Sb sites that are located far from Ru. Third, and most importantly, below $T \sim 1$ K, $1/T_1^S$ is proportional to T ; the magnitude of $1/T_1^S T$ increases with increasing x .

The $1/T_1^S T = \text{const}$. relation indicates that a finite DOS is induced by the impurity. $1/T_1$ in the superconducting state may be expressed as

$$\frac{T_1(T = T_c)}{T_1} = \frac{2}{k_B T_c} \int (N_s(E)^2 + M_s(E)^2) f(E)(1 - f(E)) dE, \quad (2)$$

where $N_s(E) = N_0 E / (E^2 - \Delta^2)^{1/2}$ is the superconducting DOS with Δ being the superconducting gap, $M_s(E) = N_0 \Delta / (E^2 - \Delta^2)^{1/2}$ is the anomalous DOS due to the coherence factor,²⁹ N_0 is the DOS in the normal state and $f(E)$ is the Fermi function. In the $T=0$ limit, $1/T_1$ is dominated by $N_s(0)^2$. The present results indicate that $N_s(0)$ is finite in the Ru-doped samples and increases with increasing x . This result cannot be accounted for by an s -wave gap.^{18–20} It is emphasized that only if there is a sign change in the gap function, namely, there are nodes in the gap function, can the impurity induce the finite DOS.²⁰ Thus, our results provide strong evidence for the existence of nodes in the gap function. The seemingly expo-

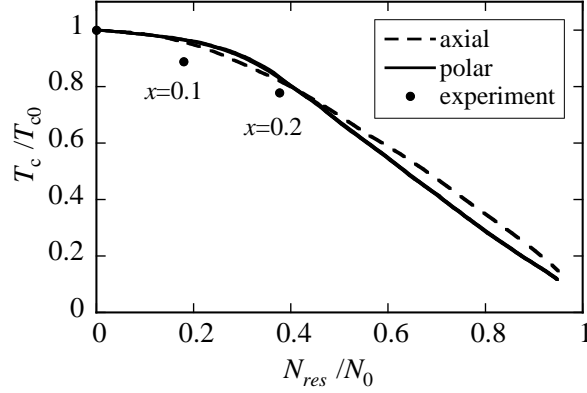


Fig. 4. Suppression of T_c as a function of the residual DOS induced by the impurity, where T_{c0} is the transition temperature in the absence of impurity scattering. The curves indicate the calculated results obtained by Miyake.^{21,22}

nential decrease in $1/T_1$ with respect to T in pure $\text{PrOs}_4\text{Sb}_{12}$ may be an effect obscured by the double superconducting transitions.^{30,31} Let us now estimate the impurity-induced $N_s(0)$, denoted as N_{res} hereafter. The values of N_{res} calculated from the relation of

$$\frac{N_{res}}{N_0} = \sqrt{\frac{(T_1^s T)_{T_c}}{(T_1^s T)_{low-T}}} \quad (3)$$

are shown in Fig. 4. The curves indicate the calculated results obtained by Miyake for the gaps with line-nodes (axial) and point-nodes (polar).^{21,22} The experimental results agree qualitatively with the theoretical results. That the experimental data fall below the theoretical curve is probably due to the depression of the pairing force by the substitution of Ru, which is not included in the theoretical results. We will discuss this point later. Although we are unable to distinguish between line nodes and point nodes in Fig. 4, point nodes nonetheless seem more plausible, in view of the relatively weaker suppression of T_c by the impurity with respect to x .²³

For completeness, we show the temperature dependence of $1/T_1^L$ in Fig. 5. Above T_c , $1/T_1^L$ shows a temperature variation very close to that of $\text{PrRu}_4\text{Sb}_{12}$. This $1/T_1^L$ can be assigned to come from the Sb sites that are located close to Ru. Below T_c , $1/T_1^L$ decreases rapidly, with no coherence peak.

Finally, we discuss the high-temperature behavior of $1/T_1^S$. Figure 6 shows the temperature variation of the quantity $1/T_1 T$. Below $T \sim 6$ K, $1/T_1 T$ decreases, leaving a peak at around $T \sim 6$ K. Such a decrease becomes mild as x increases. Since the CEF gap Δ_{CEF} is small, Kotegawa *et al.* have analyzed the low- T data by decomposing $1/T_1 T$ into two parts,¹³ namely, the contribution due to the excitation to the $\Gamma_4^{(2)}$ state, and that due to heavy quasiparticles: $1/T_1 T = \alpha \times \exp(-\Delta_{CEF}/k_B T) + \beta \times 0.7 \text{ s}^{-1} \text{ K}^{-1}$, where $0.7 \text{ s}^{-1} \text{ K}^{-1}$ is the $1/T_1 T$ for $\text{LaOs}_4\text{Sb}_{12}$ and the parameter $\sqrt{\beta}$ represents the mass enhancement factor of the heavy quasiparticles.

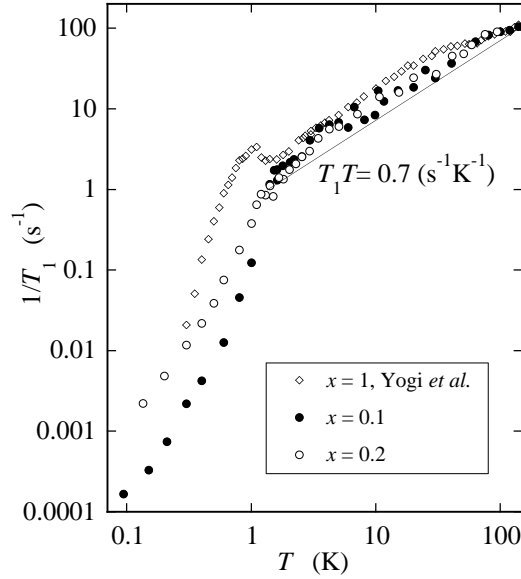


Fig. 5. Temperature dependence of the minor, slow relaxation component, $1/T_1^L$. The straight line indicates the $1/T_1 T = 0.7 \text{ s}^{-1} \text{ K}^{-1}$ relation found in $\text{LaOs}_4\text{Sb}_{12}$.

The application of the same analysis of Kotegawa *et al.* to the $x=0.1$ and 0.2 samples, as shown in the inset of Fig. 6, shows that Δ_{CEF} increases with increasing x , while β decreases with increasing x . The results are summarized in Table I, which are in good agreement with those reported by Frederick *et al.* who deduced Δ_{CEF} from the susceptibility and the mass enhancement factor from the specific heat coefficient γ .²³ As has been discussed by several authors,^{14,23} the increase in Δ_{CEF} is responsible, at least partly, for the decrease in T_c in going from $\text{PrOs}_4\text{Sb}_{12}$ to $\text{PrRu}_4\text{Sb}_{12}$; thus, the discrepancy between the theoretical curve and the experimental data seen in Fig. 4 can be ascribed to the increase in Δ_{CEF} .

In conclusion, we have studied the impurity effect on the superconductivity in the filled skutterudite heavy fermion superconductor $\text{PrOs}_4\text{Sb}_{12}$ using the NQR technique. We find that replacing Os with Ru brings about a finite density of states at the Fermi level, which increases with increasing Ru content. Our results provide strong evidence for the existence of nodes in the gap function.

Acknowledgment

We are grateful to Y. Kitaoka, H. Kotegawa, Yogi and Y. Imamura for helpful discussions and contribution. We would also like to thank K. Miyake for providing the unpublished calculated results shown in Fig. 4. This work was supported in part by a research grant from MEXT on the Priority Area “Skutterudites” (No. 15072204).

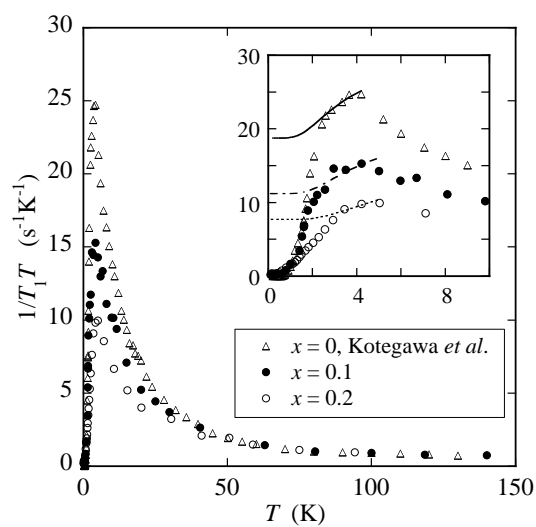


Fig. 6. Temperature dependence of the quantity $1/T_1^S T$. The inset shows the enlarged part below $T=10$ K. The curves indicate the results of fitting $1/T_1^S T = \alpha \times \exp(-\Delta_{CEF}/k_B T) + \beta \times 0.7$ $s^{-1}K^{-1}$. For details, see the text.

References

- 1) E. D. Bauer, N. A. Frederick, P.-C. Ho, V. S. Zapf and M. B. Maple: Phys. Rev. B **65** (2002) 100506.
- 2) M. B. Maple, P.-C. Ho, V. S. Zapf, N. A. Frederick, E. D. Bauer, W. M. Yuhasz, F. M. Woodward, and J. W. Lynn: J. Phys. Soc. Jpn. **71** (2002) Suppl. 23.
- 3) H. Sugawara, S. Osaki, S. R. Saha, Y. Aoki, H. Sato, Y. Inada, H. Shishido, R. Settai, Y. Onuki, H. Harima and K. Oikawa: Phys. Rev. B **66** (2002) 220504(R).
- 4) Y. Aoki, T. Namiki, S. Ohsaki, S. R. Saha, H. Sugawara and H. Sato: J. Phys. Soc. Jpn. **71** (2002) 2098.
- 5) K. Tenya, N. Oeschler, P. Gegenwart, F. Steglich, N. A. Frederick, E. D. Bauer and M. B. Maple: Acta Physica Polonica B **34** (2003) 995.
- 6) T. Tayama, T. Sakakibara, H. Sugawara, Y. Aoki and H. Sato: J. Phys. Soc. Jpn **72** (2003) 1516.
- 7) M. Kohgi, K. Iwasa, M. Nakajima, N. Metoki, S. Araki, N. Bernhoeft, J. M. Mignot, A. Gukasov, H. Sato, Y. Aoki and H. Sugawara: J. Phys. Soc. Jpn **72** (2003) 1002.
- 8) K. Kuwahara, K. Iwasa, M. Kohgi, K. Kaneko, S. Araki, N. Metoki, H. Sugawara, Y. Aoki and H. Sato: J. Phys. Soc. **73** (2004) 1438 .
- 9) E. A. Goremychkin, R. Osborn, E. D. Bauer, M. B. Maple, N. A. Frederick, W. M. Yuhasz, F. M. Woodward and J. W. Lynn: Phys. Rev. Lett. **93** (2004) 157003.
- 10) D. L. Cox: Phys. Rev. Lett. **59** (1987) 1240.
- 11) N. Takeda and M. Ishikawa: Physica B **259-261** (1999) 92.
- 12) T. D. Matsuda, K. Abe, F. Watanuki, H. Sugawara, Y. Aoki, H. Sato, Y. Inada, R. Settai and Y. Ōnuki: Physica B **312-313** (2002) 832.
- 13) H. Kotegawa, M. Yogi, Y. Imamura, Y. Kawasaki, G.-Q. Zheng, Y. Kitaoka, S. Ohsaki H. Sugawara, Y. Aoki and H. Sato: Phys. Rev. Lett. **90** (2003) 027001.
- 14) M. Yogi, H. Kotegawa, Y. Imamura, G.-Q. Zheng, Y. Kitaoka, H. Sugawara and H. Sato: Phys. Rev. B **67** (2003) 180501(R).
- 15) K. Asayama, Y. Kitaoka, G. - q. Zheng, K. Ishida and Y. Tokunaga: *Annual Reports on NMR Spectroscopy* (Academic Press, London, 2001) Vol. 44, p. 75.
- 16) D. E. Maclaughlin, J. E. Sonier, R. H. Heffner, O. O. Bernal, B. -L. Young, M. S. Rose, G. D. Morris, E. D. Bauer, T. D. Do and M. B. Maple: Phys. Rev. Lett. **89** (2002) 157001.
- 17) K. Izawa, Y. Nakajima, J. Goryo, Y. Matsuda, S. Osaki, H. Sugawara, H. Sato, P. Thalmeier and K. Maki: Phys. Rev. Lett. **90** (2003) 117001.
- 18) L. Yu: Acta Phys. Sinica **21** (1965) 75.
- 19) H. Shiba: Prog. Theor. Phys. **40** (1968) 435.
- 20) R. Fehrenbacher and M. R. Norman: Phys. Rev. B **50** (1994) 3495.
- 21) S. Schmitt-Rink, K. Miyake, and C. M. Varma: Phys. Rev. Lett. **57** (1986) 2575
- 22) K. Miyake: unpublished.
- 23) N. A. Frederick, T. D. Do, P.-C. Ho, N. P. Butch, V. S. Zapf and M. B. Maple: Phys. Rev. B **69** (2004) 024523.
- 24) E. E. M. Chia, M. B. Salamon, D. Vandervelde, D. Kikuchi, H. Sugawara and H. Sato: Cond-mat/0411395.
- 25) A. Abragam: *The Principles of Nuclear Magnetism* (Oxford Univ. Press, London, 1961).
- 26) G.-Q. Zheng, N. Yamaguchi, H. Kan, Y. Kitaoka, J. L. Sarrao, P. G. Pagliuso, N. O. Moreno and

- J. D. Thompson: Phys. Rev. B **70** (2004) 014511.
- 27) J. Chepin and J. H. Ross: J. Phys. Condens. Matt. **3** (1991) 8103.
- 28) H. Harima: unpublished.
- 29) D. E. Maclaughlin: *Solid State Physics*, eds. H. Ehrenreich *et al.* (Academic Press, New York, 1976) Vol. 31, p. 1.
- 30) R. Vollmer, A. Faißt, C. Pfeiderer, H. V. Löhneysen, E. D. Bauer, P.-C. Ho, V. Zapf and M. B. Maple: Phys. Rev. Lett. **90** (2003) 057001.
- 31) M.-A. Measson, D. Braithwaite, J. Flouquet, G. Seyfarth, J. P. Brison, E. Lhotel, C. Paulsen, H. Sugawara and H. Sato: Phys. Rev. B **70** (2004) 064516.